Solution Processing and Resist-Free Nanoimprint Fabrication of Thin Film Chalcogenide Glass Devices: Inorganic–Organic Hybrid Photonic Integration

Yi Zou, Loise Moreel, Hongtao Lin, Jie Zhou, Lan Li, Sylvain Danto, J. David Musgraves, Erick Koontz, Kathleen Richardson, Kevin D. Dobson, Robert Birkmire, and Juejun Hu*

Organic polymer materials are widely credited with extreme versatility for thin film device processing. However, they generally lack the high refractive indices of inorganic semiconductors essential for tight optical confinement in planar integrated photonic circuits. Inorganic–organic hybrid photonic systems overcome these limits by combining both types of materials, although such hybrid integration remains challenging given the vastly different properties of the two types of materials. In this paper, a new approach is used to realize inorganic–organic hybrid photonics using chalcogenide glass (ChG) materials. Known as an amorphous semiconductor, the glass possesses high refractive indices, and can be prepared in a thin film form through solution deposition and patterned via direct thermal nanoimprinting, processing methods traditionally exclusive to polymer materials only. Sub-micrometer waveguides, microring resonators, and diffraction gratings fabricated from solution processed (SP) ChG films can be monolithically integrated with organic polymer substrates to create mechanically flexible, high-index-contrast photonic devices. The resonators exhibit a high quality factor (Q-factor) of 80 000 near 1550 nm wavelength. Free-standing, flexible ChG gratings whose diffraction properties can be readily tailored by conformal integration on nonplanar surfaces are also demonstrated.

1. Introduction

Polymers have been considered a promising material for on-chip integrated photonics since they are amenable to highly versatile, scalable, and cost-effective thin film device processing. Unlike inorganic semiconductor photonic devices which require complicated multi-step processing, including vacuum growth, fine-line lithography and plasma etching, polymer films can be deposited on most technically important substrates, free of lattice matching constraints, using spin coating, dip coating, spray deposition, or electrospinning, and photonic devices can be subsequently defined using soft lithography methods such as elastomer nanoimprint with sub-micrometer resolution.[1] These solution-based methods claim the advantages of low-cost, reduced facility requirements, and compatibility with roll-to-roll processing on nonplanar and plastic substrates.[2] Despite the processing benefits, optical polymers typically have low refractive indices between 1.5 and 1.6,[3] and the low refractive indices cannot offer sufficient index contrast for strong optical confinement essential for high-density photonic integration. An inorganic–organic high refractive index polymer (HRIP) nanocomposite consisting of inorganic nanoparticles (e.g. TiO_2, ZnO, ZnS, or ZrO_2 nanoparticles) embedded in a polymer matrix forms an effective medium with refractive index up to 2.0.[4] However, nanoparticle aggregation and scattering loss remain as key challenges towards their applications in guided wave optics.[5]

Here we demonstrate a novel method of creating hybrid inorganic-organic photonic devices using SP ChG materials. Known as an amorphous semiconductor,[6] ChGs feature high refractive indices up to 3.5, much higher than those of HRIP

Y. Zou, L. Moreel, H. Lin, J. Zhou, L. Li, Prof. R. Birkmire, Prof. J. Hu
Department of Materials Science & Engineering
University of Delaware
Newark, Delaware 19716, USA
E-mail: hujuejun@udel.edu

Dr. S. Danto
ICMCB-Department of Chemistry
University of Bordeaux
33000, Bordeaux, France

Dr. J. D. Musgraves
IRradiance Glass, Inc.
Orlando, Florida 32816, USA

E. Koontz
Department of Materials Science and Engineering
Clemson University
Clemson, SC 29634, USA

Prof. K. Richardson
The College of Optics & Photonics
Department of Materials Science and Engineering
University of Central Florida
Orlando, Florida 32816, USA

Dr. K. D. Dobson, Prof. R. Birkmire
Institute of Energy Conversion
University of Delaware
Newark, DE 19716, USA

**ADVANCED
OPTICAL
MATERIALS**
www.advopticalmat.de

**Materials
Views**
www.MaterialsViews.com

nanocomposites.[7] Notably, a recent surge of interest in solution-derived ChGs shows that these glasses can be dissolved in amine solutions (in particular, ethylenediamine) through a Lewis acid–base chelation reaction.[8] Upon solvent removal through annealing, solution-derived glasses can re-polymerize to form 2D chain-like or 3D interconnected network structures comprising of covalently bonded atoms resembling those of parent bulk glasses. Rheologically similar to solution-deposited organic polymers, solution-derived ChGs are replacing polymers in emerging applications such as optical adhesives, where their high refractive indices minimize reflection between inorganic optical components. A salient example is the adoption of SP As_2Se_3 films in stacked solar cells as inter-layer adhesives, which led to the recent demonstration of solar cells with an energy conversion efficiency of 44%.[9] In addition, SP ChGs are also amenable to soft lithographic patterning methods such as micromolding in capillaries[10] and microtransfer molding.[11] In this paper, we combined solution deposition of ChG thin films and elastomer-based "soft" nanoimprint to fabricate high-index-contrast integrated photonic devices in ChG thin films. We chose the nanoimprint approach given its superior resolution (~25 nm)[1a] compared to other soft lithography techniques, which is critical to the fabrication of low-loss high-index-contrast photonic structures. Thermal nanoimprint has been applied to patterning of large-core waveguides and gratings in bulk ChGs and thermally evaporated (TE) thin films on silicon substrates.[12] Here we present the first effort to exploit nanoimprint to produce sub-micrometer waveguides

and micro-ring resonators from SP ChG films. The low processing temperature resulting from the unique rheological properties of SP ChG films allows monolithic integration on different organic polymer substrates without compromising the material's optical quality. Further, our single-step nanoimprint protocol directly molds ChG films into desired device geometries without resorting to extra pattern transfer steps, enabling seamless process integration with organic polymer photonics.
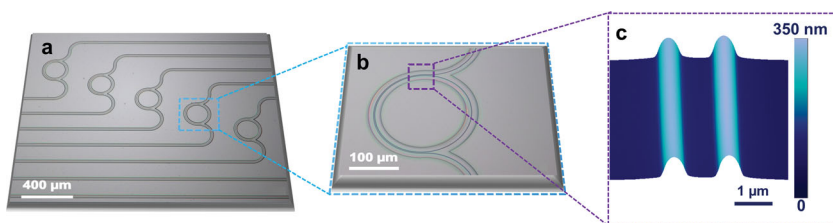
In this article, optical waveguides, microring resonators and optical gratings with sub-micrometer dimensions were fabricated in SP films deposited polymer substrates to validate our technique as a viable processing route for inorganic–organic hybrid photonic devices. A systematic analysis on the structural, chemical, and optical properties of SP As_2Se_3 ChG films included in the Supporting Information section suggests that the SP films exhibit identical structures and properties regardless of the substrate type they are deposited on, which ensures our processing reproducibility and consistency on the different polymer substrate platforms we used in this study.

2. Hybrid Devices Derived from SP As_2Se_3 Films

The hybrid devices presented in this paper were fabricated using a thermal nanoimprint process. Details of the experimental protocols can be found in the Experimental Section and are also schematically illustrated in **Figure 1**. One important distinction we want to highlight here is the significant
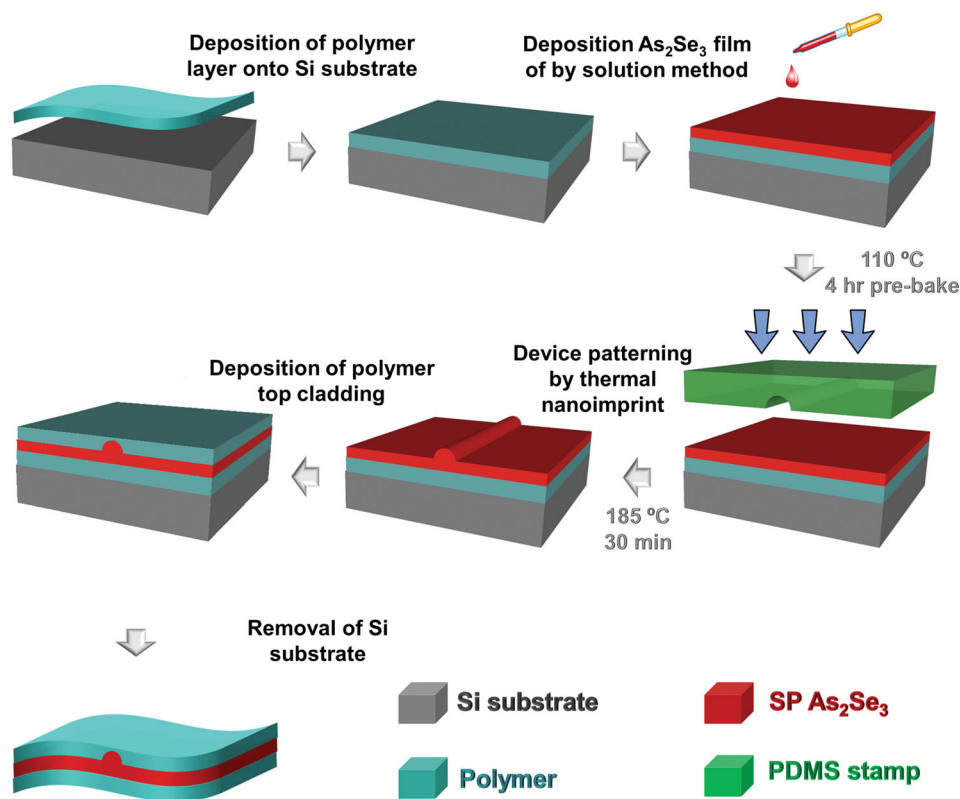
Figure 1. Schematic process flow of ChG film solution deposition and nanoimprint patterning. (not drawn to scale)

Materials
Views
www.MaterialsViews.com

ADVANCED
OPTICAL
MATERIALS
www.advopticalmat.de

FULL PAPER

Figure 2. Imprinted ring resonators on flexible polymer substrates. (a,b) Top-view microscope images of imprinted microring resonators with radii of 100 μm; (c) surface morphology of a coupling section between a bus waveguide and a microring measured by AFM. The waveguides exhibit an RMS line-edge roughness of 0.9 nm. The coupling gap width is 1 μm.

thermal property difference between SP ChG films and those obtained by thermal evaporation, which were also amenable to imprint fabrication.[12h] After spin coating, the SP films were pre-baked at 110 °C, much lower than the typical baking temperature of 140–170 °C required to remove the amine solvent.[8c] The residual solvent in SP films after pre-bake results in its decreased softening temperature compared to TE films, which kinetically facilitates viscous flow of glass to fill the stamping mold during imprint. For instance, we were unable to imprint sub-micrometer photonic devices using TE As$_2$Se$_3$ films even at elevated temperatures up to 250 °C (and otherwise identical imprint conditions) when the PDMS elastomer stamp begins to denature. This unique property of SP films is critical to maintaining imprinted pattern fidelity at reduced processing temperatures necessary for inorganic-organic integration.

Using the solution deposition and nanoimprint method, we fabricated high-index-contrast (SP As$_2$Se$_3$ film has a high reflective index of 2.7 around 1550 nm wavelength), free-standing and mechanically compliant glass-polymer hybrid photonic devices on flexible SU-8 epoxy, polyimide, and PET substrates. **Figure 2**a and b are optical microscope images showing pulley-coupled micro-rings resonators on an SU-8 epoxy membrane delaminated from a silicon substrate. Atomic force microscopy (AFM) measurements on these devices shown in Figure 2c yield a smooth surface finish of the imprinted devices with a low root mean square (RMS) line-edge roughness of (0.9 ± 0.2) nm. **Figure 3**b plots the measured transmission spectrum of a flexible micro-ring resonator on a free-standing SU-8 membrane near 1520 nm wavelength. The flexible resonators exhibited an intrinsic quality factor (Q-factor) of (80 000 ± 10%), which was fitted from the transmission spectra using standard protocols[12h] and averaged over three devices. This Q-factor corresponds to an equivalent waveguide propagation loss of (6.0 ± 0.6) dB/cm, comparable to previous reports on waveguides fabricated from SP ChG films.[10,13] Given the sub-nm surface roughness and hence negligible scattering loss, we conclude that this observed loss results from optical absorption by the residual ethylenediamine (EDA) solvent, which contains N–H bonds that have an overtone absorption around 1510 nm. The presence of residual solvent in SP films after the imprint process is further supported by our Fourier transform infrared (FTIR) spectroscopic measurement results detailed in the Supporting Information. Optical loss caused by solvent residue is also evidenced by our UV-Vis transmission measurements detailed in the Supporting Information. In comparison, resonator devices with identical configurations, but imprinted from

TE As$_2$Se$_3$ films, claim a higher Q-factor up to 4×10^5 since such parasitic solvent absorption is absent.[12h] Due to the stable chelate bondings between the EDA ligand and the As atom, EDA solvent residue persists even after post-deposition annealing.[8c] Therefore, it is not possible to suppress the optical loss via simple heat treatment. However, switching to a different solvent mixture with reduced EDA load may contribute to loss mitigation.[8b] We further note that the 80 000 intrinsic Q is sufficient for a broad range of photonic applications where tens-of-centimeters-long optical path length is not required: the examples include optical adhesives, multi-layer Bragg reflectors and cavities, refractometry sensors, light trapping/extraction structures for solar cells and infrared LEDs, as well as diffractive optical elements which we will present in the following paragraph.

We further demonstrated successful imprint fabrication of SP As$_2$Se$_3$ gratings on flexible PET and polyimide substrates (**Figure 4**a,b). We choose PET and polyimide substrates over SU-8 for grating fabrication as they have better mechanical
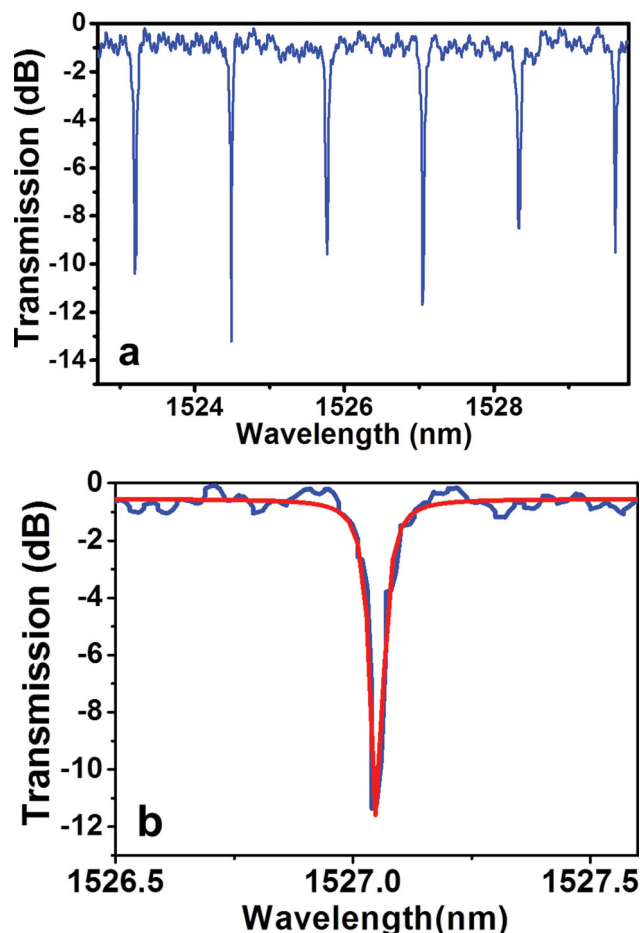
Figure 3. Optical characterizations of imprinted resonator devices from SP As$_2$Se$_3$ glass film. (a) Transmission spectrum of an imprinted SP As$_2$Se$_3$ microring resonator on a flexible SU-8 membrane; (b) an average intrinsic Q-factor of 80 000 was measured from the transmission spectrum.
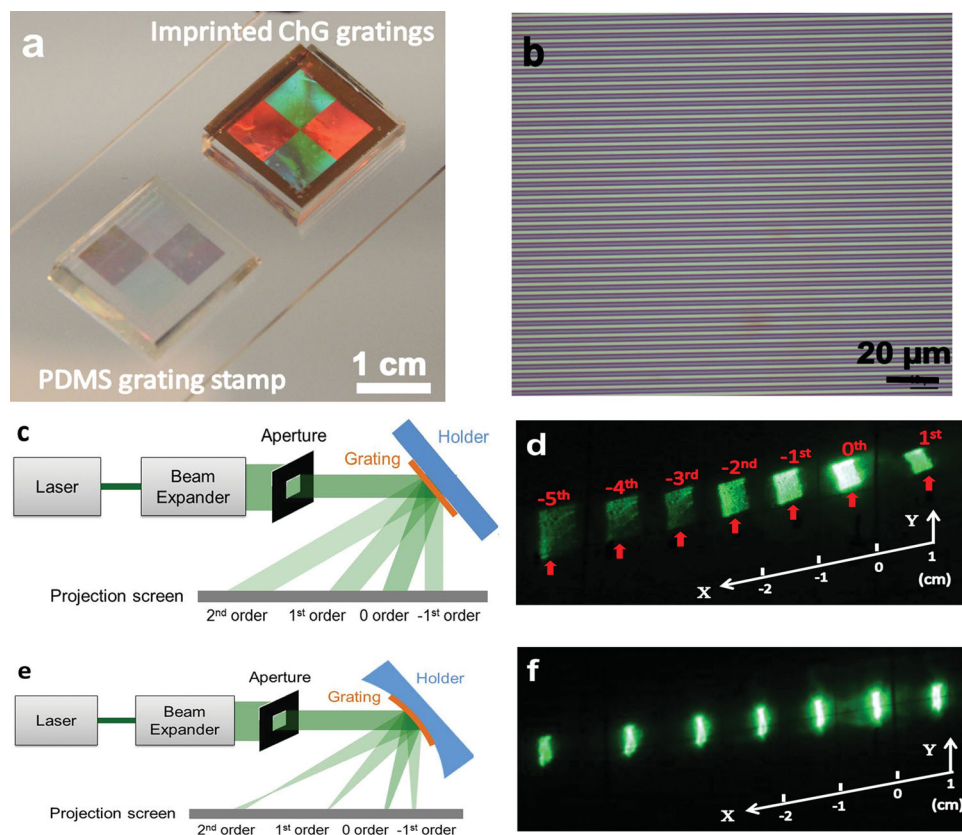
Figure 4. (a) A photo showing a PDMS grating and an imprinted As_2Se_3 grating on a flexible PET substrate under identical illumination conditions. Compared with the PDMS grating, the large index contrast of the hybrid As_2Se_3-PET grating leads to enhanced diffraction efficiency and high color saturation; (b) a top-view microscope image of the imprinted hybrid As_2Se_3-polyimide showing the well-defined line patterns with a 3 μm period; (c) schematic diagrams illustrating the experimental setup used to map the diffracting patterns from the imprinted hybrid As_2Se_3-polyimide gratings, which were attached onto a flat sample holder; (d) diffraction patterns of a collimated and expanded 532 nm green laser beam by a flexible As_2Se_3-polyimide grating (5 μm period) attached to a flat surface. The red arrows indicate the diffraction spot positions calculated using the Bragg equation; (e) schematic diagrams illustrating the experimental setup used to map the diffracting patterns from the imprinted hybrid As_2Se_3-polyimide gratings, which were attached onto a curved sample holder; (f) diffraction patterns of the same As_2Se_3-polyimide grating mounted on a curved surface (radius = 50 cm). The multi-line patterns are clearly indicative of the combined focusing and diffractive capabilities of the concave grating.

robustness. ChGs are ideal materials for gratings since their high refractive indices and low optical loss (compared to metals) lead to superior diffraction efficiency. To illustrate the effect, Figure 4a presents a photo which gives a side-by-side comparison of two gratings made of PDMS polymer and SP As_2Se_3 films but otherwise identical. The gratings were each divided into four quadrants with perpendicular orientations. The enhanced diffraction efficiency of the As_2Se_3 grating is evident from its much higher color saturation.

In addition to its improved diffraction efficiency, the As_2Se_3 grating also features adjustable diffraction characteristics by conformally attaching the grating to substrates with varying geometries. For example, a concave reflective grating combines both diffraction and imaging functions in a single element and constitutes an important component in advanced spectrophotometer and laser designs.[14] Traditional concave grating fabrication methods involve mechanical ruling or specialty optical lithography on a curved surface.[15] Our method offers a much simpler alternative for concave grating fabrication; moreover, curvature of the flexible hybrid As_2Se_3-polyimide grating can be readily defined by mechanical deformation. To demonstrate

this unique property of our flexible grating, we performed diffraction measurements using a setup schematically depicted in Figure 4c,e. A hybrid As_2Se_3-polyimide grating with 5 μm period was attached to sample holders with flat or curved surfaces. A collimated and expanded 532 nm green laser beam passed through a square aperture and was obliquely incident on the grating. The resulting diffraction pattern of the grating was recorded on a projection screen. When the grating was attached onto a flat surface, the diffracted spots maintained the square shape inherited from the aperture (Figure 4c). When the same grating was mounted on a curved resin holder (fabricated using 3D printing with a pre-defined radius of curvature of 50 cm), the square spots were transformed into a set of lines due to the focusing effect of the concave grating (Figure 4d). Note that since we used a flat projection screen, the line pattern image was not perfect when the paraxial condition was not met, which, however, can be corrected by adopting an aspherical imaging system or grating apodization. The red arrows in Figure 4d represent the x-axis positions of the diffraction spots calculated using the Bragg equation, which nicely matches the experimental results. Bending tests further indicated that

gratings on polyimide film can be uniaxially bent down to 1 mm radius without visible crack formation upon microscope inspection (see the Supporting Information). While extensive mechanical reliability and fatigue testing of these flexible structures are outside the scope of this paper, our recent results have demonstrated robust flexible glass photonic devices that can sustain repeated sub-millimeter bending cycles with minimal optical performance degradation by adopting a new multi-neutral-axis mechanical design.[16]

3. Conclusions

We have presented solution-derived chalcogenide glasses as a promising material candidate for organic–inorganic hybrid photonic device fabrication. In this study, high-index (n = 2.7) As_2Se_3 ChG films were prepared by solution deposition and patterned into functional photonic devices using direct nanoimprint, both of which are methods traditionally employed for polymer processing. We further show that SP ChG processing involves reduced thermal budget compatible with organic polymers and can potentially be seamlessly integrated into organic device fabrication processes. The method is capable of sub-micrometer pattern generation with superior fidelity and sub-nm surface roughness. We used the technique to demonstrate ChG resonators integrated on flexible polymer substrates and the resulting devices exhibit a high intrinsic Q-factor of 80 000 near 1550 nm wavelength. We also use the approach to demonstrate hybrid As_2Se_3-polyimide diffractive gratings whose diffractive properties can be readily adjusted by mechanical deformation. The glass-polymer hybrid photonics technology is expected to open up a versatile fabrication route for unconventional device architectures ranging from mechanically deformable optical elements to light management nanostructure for organic photonics.

4. Experimental Section

Chalcogenide Glass Film Deposition: bulk As_2Se_3 glass (IRradiance glass. Inc.) was prepared using a traditional melt-quenching technique. More details regarding the bulk glass preparation process can be found from prior reports.[17] Solutions of As_2Se_3 were prepared by dissolving ground As_2Se_3 glass powders into ethylenediamine (Fluka Chemicals, ≥99.5%). The dissolution process was carried out inside a sealed glass container to prevent solvent evaporation. A hot plate with magnetic stirrer was used to expedite the dissolution process. The solution was then centrifuged at 4000 rpm for 10 min and filtered using syringe filters with 0.2 micrometer filtration membranes to remove suspended particles and insoluble impurities. Spin-coating was conducted in a nitrogen-purged glove box to prevent oxygen and water contamination. Glass solution with desired concentrations of As_2Se_3 was pipetted onto various substrates including SU-8 (MicroChem Inc.) coated glass slides or silicon substrates (Universitywafers Inc.), PET films (100 μm thick, Goodfellow Inc.) and polyimide films (50 μm thick, Umeco Inc.), and spun at various rates for 30 s. The resulting films were annealed in a vacuum oven heating at 110 °C for 4 h. Micro-ring resonators and gratings were imprinted from 360 nm-thick films prepared from a solution with 0.2 g/mL glass loading and at a spin rate of 3000 rpm. As_2Se_3 films deposited by thermal evaporation were used for baseline comparison in material characterizations. More details concerning the film thermal evaporation process may be found elsewhere.[8c]

Preparation of PDMS Composite Sstamps: an NR9–1000PY photoresist (Futurrex inc.) pattern was first defined on a Si wafer using contact photolithography on a Karl Suss MJB-3 mask aligner, and then a thermal treatment at 130 °C for 10 s was implemented to reflow the NR9 polymer resist and create a smooth surface finish. This photoresist pattern was used as the master mold and can be conveniently used many times (>20 times in our experiments) as the template to replicate PDMS composite stamps. PDMS composite stamps were fabricated as follows: a solution was prepared by mixing 2 g of vinylmethylsiloxane-dimethylsiloxane trimethylsiloxy terminated copolymer (VDT-731, from Gelest Inc.) with 0.2 g of Sylgard 184 curing agent (Dow Corning Inc.) and 0.02 mL of platinum catalyst (Gelest Inc.). After degassing in a desiccator, the bubble-free mixture was spin-coated onto the master mold at 3000 rpm for 30 s and then pre-baked at 100 °C for 1 min. The second layer is made by casting liquid PDMS (Sylgard 184, Dow Corning Inc., 10:1 mixing ratio between the monomer and the curing agent) onto the pre-coated master mold. The bilayer composite mold was baked at 80 °C for 4 h and then baked at 110 °C for 1 h to ensure that the PDMS was fully cured. More details concerning the preparation of PDMS composite stamps may be found elsewhere.[18]

Device Patterning by Thermal Nanoimprinting: a schematic of the nanoimprint process flow is shown in Figure 1. We first attached or deposited a polymer film/layer onto a polished silicon substrate either by spin coating (in the case of SU-8 epoxy) or using sticky tapes (for PET or polyimide films). The handler substrate surface was silanized prior to SU-8 coating to facilitate subsequent SU-8 delamination. ChG films were then deposited onto the polymer layer using the spin coating method and stabilized by annealing. Imprint was performed in a glove box purged by N_2 in order to prevent the chalcogenide glass film from oxidation. A glass film-stamp sample was placed on a hotplate pre-set at desired temperature. Imprint pressure (approximately 0.13 MPa) was applied by loading a metal block on the film-stamp assembly. Waveguides, resonators and gratings made from SP As_2Se_3 glass films were imprinted at 185 °C for 30 min. After imprint the sample was removed from the hotplate when it cooled to below 60 °C at a ramp-down rate of 5 °C/min. The stamp was then manually delaminated from the ChG glass sample. A 3 μm-thick SU-8 polymer (MicroChem Inc.) layer was spin coated on the patterned glass samples to serve as a top cladding which prevents the glass films from surface oxidation and a surface planarizing layer.[16a] Free-standing flexible photonic devices were completed by detaching the polymer encapsulated devices from the Si substrate.

Measurement of Surface Morphology and Roughness: the measurement was conducted using tapping mode atomic force microscopy (AFM) on a Dimension 3100 (Digital Instruments, Inc.) microscope. AFM line scans were performed parallel to the waveguides to accurately measure the waveguide line edge roughness. We ran scans at 5 or more different locations on each sample and averaged the results. The cross sectional images of imprinted waveguides/resonators were taken on a JSM-7400F (JEOL, Inc.) scanning electron microscope (SEM).

Optical Characterizations of Photonic Devices: a tunable laser (Agilent Technologies Model 81682A) operating in a step sweep mode was used to measure the transmission spectra of the waveguides and micro-ring resonators. Tapered lens-tip fibers (Nanonics Inc.) for end-fire coupling of TE-polarized light into and out of the devices were applied.

Supporting Information

Supporting Information is available from the Wiley Online Library or from the author.

Acknowledgments

FULL PAPER

[1] a) S. Y. Chou, P. R. Krauss, P. J. Renstrom, *Science* **1996**, *272*, 85; b) L. J. Guo, *Adv. Mater.* **2007**, *19*, 495; c) H. Schift, *J. Vac. Sci. Technol. B* **2008**, *26*, 458.

[2] a) S. H. Ahn, L. J. Guo, *Adv. Mater.* **2008**, *20*, 2044; b) C. Y. Chao, L. J. Guo, *J. Vac. Sci. Technol. B* **2002**, *20*, 2862; c) C. Stuart, Y. Chen, *ACS Nano* **2009**, *3*, 2062.

[3] a) H. Ma, A. K. Y. Jen, L. R. Dalton, *Adv. Mater.* **2002**, *14*, 1339; b) J. Cavagnaro, http://www.laserfocusworld.com/articles/print/volume-47/issue-9/features/polymer-optics-progress-in-plastic-optics-follows-advances-in-materials-and-manufacturing.html, accessed: September, 2013; c) L. Eldada, L. W. Shacklette, *IEEE J. Sel. Top. Quantum Electron.* **2000**, *6*, 54.

[4] a) C. M. Chang, C. L. Chang, C. C. Chang, *Macromol. Mater. Eng.* **2006**, *291*, 1521; b) C. L. Lu, Z. C. Cui, Z. Li, B. Yang, J. C. Shen, *J. Mater. Chem.* **2003**, *13*, 526; c) N. Suzuki, Y. Tomita, *Opt. Express* **2006**, *14*, 12712; d) A. H. Yuwono, B. H. Liu, J. M. Xue, J. Wang, H. I. Elim, W. Ji, Y. Li, T. J. White, *J. Mater. Chem.* **2004**, *14*, 2978; e) M. Yoshida, P. N. Prasad, *Chem. Mater.* **1996**, *8*, 235.

[5] a) M. M. Demir, K. Koynov, U. Akbey, C. Bubeck, I. Park, I. Lieberwirth, G. Wegner, *Macromolecules* **2007**, *40*, 1089; b) L. Q. Qiu, K. Saravanamuttu, *J. Opt.* **2012**, *14*.

[6] K. Tanaka, *Semiconductors* **1998**, *32*, 861.

[7] a) S. Danto, P. Houizot, C. Boussard-Pledel, X. H. Zhang, F. Smektala, J. Lucas, *Adv. Funct. Mater.* **2006**, *16*, 1847; b) V. K. Tikhomirov, D. Furniss, A. B. Seddon, J. A. Savage, P. D. Mason, D. A. Orchard, K. L. Lewis, *Infrared Phys. Technol.* **2004**, *45*, 115.

[8] a) T. Guiton, C. Pantano, *Chem. Mater.* **1989**, *1*, 558; b) Y. L. Zha, S. Fingerman, S. J. Cantrell, C. B. Arnold, *J. Non-Cryst. Solids* **2013**, *369*, 11; c) Y. Zou, H. T. Lin, O. Ogbuu, L. Li, S. Danto, S. Novak, J. Novak, J. D. Musgraves, K. Richardson, J. J. Hu, *Opt. Mater. Express* **2012**, *2*, 1723; d) T. Kohoutek, T. Wagner, M. Vlcek, M. Frumar, *J. Non-Cryst. Solids* **2006**, *352*, 1563; e) T. Kohoutek, T. Wagher, M. Vlcek, M. Frumar, *J. Non-Cryst. Solids* **2005**, *351*, 2205; f) T. Kohoutek, T. Wagner, J. Orava, M. Krbal, A. Fejfar, T. Mates, S. O. Kasap, M. Frumar, *J. Non-Cryst. Solids* **2007**, *353*, 1437; g) Y. L. Zha, C. B. Arnold, *Opt. Mater. Express* **2013**, *3*, 309; h) Y. L. Zha, P. T. Lin, L. Kimerling, A. Agarwal, C. B. Arnold, *ACS Photonics* **2014**, *1*, 153; i) Y. L. Zha, M. Waldmann, C. B. Arnold, *Opt. Mater. Express* **2013**, *3*, 1259.

[9] X. Sheng, C. Bower, S. Bonafede, J. Wilson, B. Fisher, M. Meitl, H. Yuen, S. Wang, L. Shen, S. Burroughs, J. A. Rogers, *Nat. Mater.* **2014**, DOI: 10.1038/nmat3946.

[10] C. Tsay, Y. L. Zha, C. B. Arnold, *Opt. Express* **2010**, *18*, 26744.

[11] C. Tsay, F. Toor, C. F. Gmachl, C. B. Arnold, *Opt. Lett.* **2010**, *35*, 3324.

[12] a) T. Han, S. Madden, D. Bulla, B. Luther-Davies, *Opt. Express* **2010**, *18*, 19286; b) Z. G. Lian, W. J. Pan, D. Furniss, T. M. Benson, A. B. Seddon, T. Kohoutek, J. Orava, T. Wagner, *Opt. Lett.* **2009**, *34*, 1234; c) J. Orava, T. Kohoutek, A. L. Greer, H. Fudouzi, *Opt. Mater. Express* **2011**, *1*, 796; d) W. J. Pan, H. Rowe, D. Zhang, Y. Zhang, A. Loni, D. Furniss, P. Sewell, T. M. Benson, A. B. Seddon, *Microw. Opt. Technol. Lett.* **2008**, *50*, 1961; e) M. Silvennoinen, K. Paivasaari, J. J. J. Kaakkunen, V. K. Tikhomirov, A. Lehmuskero, P. Vahimaa, V. V. Moshchalkov, *Appl. Surf. Sci.* **2011**, *257*, 6829; f) M. Solmaz, H. Park, C. K. Madsen, X. Cheng, *J. Vac. Sci. Technol. B* **2008**, *26*, 606; g) I. Yamada, N. Yamashita, K. Tani, T. Einishi, M. Saito, K. Fukumi, J. Nishii, *Opt. Lett.* **2011**, *36*, 3882; h) Y. Zou, D. Zhang, H. T. Lin, L. Li, L. Moreel, J. Zhou, Q. Y. Du, O. Ogbuu, S. Danto, J. D. Musgraves, K. Richardson, K. Dobson, R. Birkmire, J. Hu, *Adv. Optical Mater.* **2014**, DOI: 10.1002/adom.201300489; i) A. B. Seddon, W. J. Pan, D. Furniss, C. A. Miller, H. Rowe, D. Zhang, E. McBrearty, Y. Zhang, A. Loni, P. Sewell, T. M. Benson, *J. Non-Cryst. Solids* **2006**, *352*, 2515.

[13] C. Tsay, E. Mujagic, C. K. Madsen, C. F. Gmachl, C. B. Arnold, *Opt. Express* **2010**, *18*, 15523.

[14] a) W. C. Cash, *Appl. Optics* **1984**, *23*, 4518; b) S. Singh, *Opt. Laser Technol.* **1999**, *31*, 195.

[15] a) T. Harada, T. Kita, *Appl. Optics* **1980**, *19*, 3987; b) Y. J. Xie, Z. Q. A. Lu, F. Y. Li, J. L. Zhao, Z. C. Weng, *Opt. Express* **2002**, *10*, 1043.

[16] a) L. Li, H. T. Lin, S. Qiao, Y. Zou, S. Danto, K. Richardson, J. D. Musgraves, N. Lu, J. Hu, unpublished; b) L. Li, Y. Zou, H. T. Lin, J. J. Hu, X. C. Sun, N. N. Feng, S. Danto, K. Richardson, T. Gu, M. Haney, *J. Lightwave Technol.* **2013**, *31*, 4080.

[17] a) J. D. Musgraves, P. Wachtel, S. Novak, J. Wilkinson, K. Richardson, *J. Appl. Phys.* **2011**, *110*, 063503; b) L. Petit, N. Carlie, F. Adamietz, M. Couzi, V. Rodriguez, K. C. Richardson, *Mater. Chem. Phys.* **2006**, *97*, 64.

[18] C. Pina-Hernandez, V. Lacatena, G. Calafiore, S. Dhuey, K. Kravtsov, A. Goltsov, D. Olynick, V. Yankov, S. Cabrini, C. Peroz, *Nanotechnology* **2013**, *24*, 065301.